Journal of Solid State Chemistry 182 (2009) 182–186

Contents lists available at ScienceDirect

Journal of Solid State Chemistry

journal homepage: www.elsevier.com/locate/jssc

Surfactant-free fabrication of Cu_2O nanosheets from Cu colloids and their tunable optical properties

Yongsong Luo [a,*], Youchao Tu [a], Qinfeng Ren [b], Xiaojun Dai [a], Lanlan Xing [b], Jialin Li [b]

[a] *Department of Physics Electronic Engineering, XinYang Normal University, Xinyang 464000, China*
[b] *Department of Physics, Central China Normal University, Wuhan 430079, China*

ARTICLE INFO

Article history:
Received 12 June 2008
Received in revised form
23 July 2008
Accepted 23 September 2008
Available online 19 October 2008

Keywords:
Disproportionating reaction
Copper colloid
Oxidation
Cuprous oxide

ABSTRACT

Novel sheetlike Cu_2O two-dimensional (2D) nanoarchitectures were successfully synthesized via a copper nanoparticle-mediated process for the first time. Uniform and nearly monodisperse Cu nanocolloids were firstly synthesized by disproportionating reaction of Cu^+ at the surfactant-free ambient conditions, and Cu_2O nanosheets were subsequently synthesized by choosing ethanol solvent agent to limit the oxidized processes of Cu nanocolloids. The synthesized products were systematically studied by X-ray powder diffraction, scanning electron microscopy (SEM), transmission electron microscopy (TEM) and UV–vis absorption spectra. It was demonstrated that the solvent agent of ethanol played key roles in the formation of the as-synthesized nanosheets. By choosing the different solvent agents to limit the oxidized processes, Cu_2O nanospheres and nanocubes can be selectively synthesized accordingly.

1. Introduction

Nanotechnology is based on the smallest units of matter to process new materials and devices atom by atom in order to obtain superior performance on the basis of atomic-scale architecture. Thus, fabrication of nanomaterials with well-defined structures and precisely controlled sizes is crucial to the development of nanotechnology [1–4]. So far, much effort has been employed to fabricate nanomaterials with different shapes, such as nanobelts, nanowires, nanotubes, nanocubes, nanoboxes, hollow spheres, etc. [5–9]. Among all the morphologies, fabrication of complex architectures with two-dimensional (2D) or highly ordered nanostructures is highly desirable in current materials synthesis, holding the promise of advanced applications in electronics and optoelectronics [10–12]. For example, roselike nanoflower consisting of 2D ZnO nanosheets was deposited in chemical bath using layered basic acetate dehydrate for enhancing light conversion efficiency to electricity in dye-sensitized solar cells (DSCs) [13]. Three-dimensional (3D) flowerlike MoS_2 nanostructures were fabricated by a thermal evaporation process, and they exhibited good capability in field emission due to the existence of the open edges in their nanopetals [14].

As a p-type semiconductor (direct bandgap ~2.17 eV) with unique optical and magnetic properties, cuprous oxide (Cu_2O) is a promising material with potential applications in solar energy conversion, micro-/nanoelectronics, magnetic storage devices, biosensing, and catalysis [15,16]. Recently, many efforts have been devoted to the shape-controlled synthesis of Cu_2O micro- and nanocrystals, such as wires [17,18], rods [19], cubes [7,20,21], pyramids [20], flowers [22], octahedral, etc. [23,24]. These morphologies may be attributed to that the surfactant mesophases have been proved to be useful and versatile “soft” templates, which may form different conformations by self-assembly and lead to the formation of different Cu_2O nanostructures. However, it remains a great challenge to develop surfactant-free methods for solution synthesis of well-defined Cu_2O sheet like nanostructures.

Herein, we report a feasible stepwise solution-phase synthesis of sheetlike Cu_2O 2D nanoarchitectures via a copper nanoparticle-mediated process by disproportionating reaction of Cu^+. Our method involves that the newly formed Cu nanocolloids rapidly oxidized into Cu_2O nanoparticles and subsequently converted to Cu_2O nanosheets at the surfactant-free ambient condition. Sizes and morphologies controllable Cu_2O nanoarchitectures can be obtained via an oxidation of Cu colloids dispersed in suitable solvent agent. Moreover, the optical properties of Cu_2O nanosheets were investigated by UV–vis absorption spectroscopy, which displays interesting features such as a band gap transition and a slight blue-shift of band gap absorption with respect to the value for bulk Cu_2O.

2. Experimental

All the chemicals were analytic grade reagents used without further purification. In a typical procedure, 10 ml deionized water

---

* Corresponding author. Fax: +86 376 6391732.
E-mail address: ysluo@mail2.xytc.edu.cn (Y. Luo).

0022-4596/$ - see front matter © 2008 Elsevier Inc. All rights reserved.
doi:10.1016/j.jssc.2008.09.027

was gradually (2 ml/min) added to 5 ml $TiCl_4$ which was cooled with iced bath under continuous stirring. Then, 0.9 g copper foil was added to 15 ml of $TiCl_4$ hydrolyzed solution; an inert gas environment was required to stabilize the precursor. As the aging process continued, the above mixed solution was gradually turned into Cu nanocolloids. Finally, Cu_2O nanosheets were obtained by injecting 0.5 ml of the above Cu colloids into 10 ml ethanol. In this experiment, other Cu_2O nanocrystals were also prepared for comparison by injecting 0.5 ml of the above Cu colloids into 10 ml deionized water or acetone under the same conditions.

The as-prepared sample was characterized by X-ray diffraction (XRD) on a Rigaku-DMax 2400 diffractometer equipped with the graphite monochromatized Cu$K\alpha$ radiation. Scanning electron microscopy (SEM) images were obtained on a JSM-6700F microscope operated at 5 kV. Transmission electron microscopy (TEM) observations were carried out on a JEOL JEM-2010 instrument in bright field (operated at 200 kV). The UV–vis spectra of the colloids were recorded with a UV–vis spectrophotometer (Shimadzu UV–2550).

3. Results and discussion

Sheetlike Cu_2O nanoarchitectures were synthesized via a copper nanocolloid-mediated process by disproportionating reaction of Cu^+ at surfactant-free ambient condition. In this work, we introduce ethanol as the oxidants and solvents; the chemical reaction is as follows:

$$Cu^0 + Ti^{IV} \rightarrow Cu^I + Ti^{III}$$

$$2Cu^I \rightarrow Cu^0 + Cu^{II}$$

$$Cu^{II} + Ti^{III} \rightarrow Cu^I + Ti^{IV}$$

$$4Cu^0 + O_2 \rightarrow 2Cu_2O$$

The X-ray powder diffraction (XRD) pattern of the sheetlike Cu_2O nanostructures is displayed in Fig. 1c. All of the diffraction peaks can be indexed according to the cubic phase of Cu_2O with a lattice constant $a = 4.4267$ Å, which is consistent with the value in the standard card (PDF file No.05-0667), and the results also show that the oxidation process of the Cu-based colloids is from Cu to Cu_2O. Initially, the colloidal solution exhibited the diffraction peaks of the pure Cu elements (Fig. 1a). After 30 min, the diffraction peaks of Cu_2O nanostructures appeared and accompanied with the Cu elements (Fig. 1b). Lastly, the Cu elements completely vanished and were converted to Cu_2O nanoarchitectures when the reaction time was prolonged to 60 min (Fig. 1c).

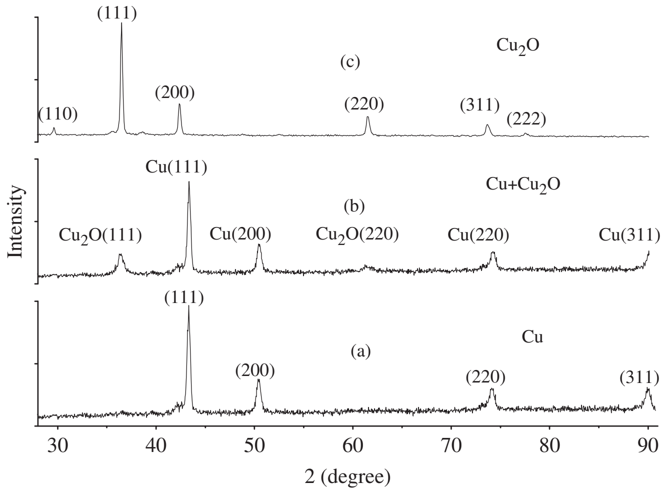

Fig. 1. XRD results of the Cu/Cu_2O nanoarchitectures. (a) Cu nanocolloids. (b) Cu/Cu_2O compound. (c) Cu_2O nanosheets.

Fig. 2a shows the uniform and nearly monodisperse Cu_2O nanosheets which could be obtained in large quantities. From the SEM observations, it can be seen that the Cu_2O product contains numerous sheet-like nanoarchitectures, and almost all of them show the same morphology. In addition, each sheet is made up of many thin nanoparticles. The sizes of these nanosheets are in the range of 200–400 nm and about 10 nm in thickness (Fig. 2b). The structures of the nanosheet were further investigated by TEM (Fig. 2c–e). Fig. 2e shows the TEM image of an individual Cu_2O nanosheet. From this image, it can be seen that the edge of the Cu_2O nanosheet is composed of many little particles, Moreover, the uniform thickness of nanosheets is also confirmed by Fig. 2e. The inset of Fig. 2e shows the typical high-resolution transmission electron microscopy (HRTEM) image of an individual Cu_2O nanosheet; the image clearly reveals that the Cu_2O nanosheet is single crystal in nature. The fast Fourier transform (FFT) pattern of Fig. 2 is displayed in the inset of Fig. 2d. The result also indicates that the assembled nanosheet is single crystal and can be indexed as the cubic phase Cu_2O, which is in accord with the XRD result in Fig. 1c.

It is intriguing to note that the nanosheets are assembled by oriented attachment of basic particles in the absence of any surfactants or templates; their growth process has been followed by examining the products harvested at different intervals of aging times. The obvious evolutionary stages can be clearly observed and are shown in Fig. 3. Initially, the uniform nanocrystals of copper colloids were obtained from solution by disproportionating reaction of Cu^+ (Fig. 3a). Then, Cu_2O structures with approximate sheet shapes appeared on injecting 0.5 ml of the above Cu colloids into 10 ml ethanol (Fig. 3b). After the aging time was increased to 60 min, most of the obtained products were perfect nanosheets, and almost no Cu_2O nanoparticles could be observed, as shown in Fig. 3c. For comparison, the other morphologies of Cu_2O nanostructures were obtained by injecting 0.5 ml of the above Cu colloids into 10 ml deionized water or acetone under the same conditions. Fig. 3d and e shows that different oxidants produce apparently different shapes of Cu_2O nanostructures (sphere, cube). Based on the results discussed above, we believe that ethanol plays a key role in the formation of the as-synthesized product. The formation of the Cu_2O nanosheets can be rationally expressed as a kinetically controlled Ostwald ripening mechanism. In our system, the medium solution may be used as the oxidant reagent; the different solutions have contained the different quantity of oxygen which would determine the speed of oxidation and produce the different morphologies of Cu_2O. When the precursor solution is added to the ethanol solution, the colloids can be quickly oxidized and further grow into nanoplates in this stage. After a longer aging time, because of the intrinsic tendency for the nucleation growth along the 2D direction due to anisotropic crystal structure, the sheetlike 2D nanoarchitectures are formed. The process of the shape transition from nanoparticles to nanosheets is summarized in Fig. 4.

UV–vis absorption measurement is one of the most important methods to reveal the energy structures and optical properties of semiconductor nanocrystals and has been studied extensively. The use of optical far-field methods for studying the morphology and physical–chemical properties of nanostructures is promising because of their speed and low cost. In our measurements, Fig. 5a shows the UV–vis spectra of 0.5 ml copper colloids dispersed in 10 ml ethanol solvents. At the initial stage of the reaction period from Cu nanocolloids to Cu_2O nanosheets,

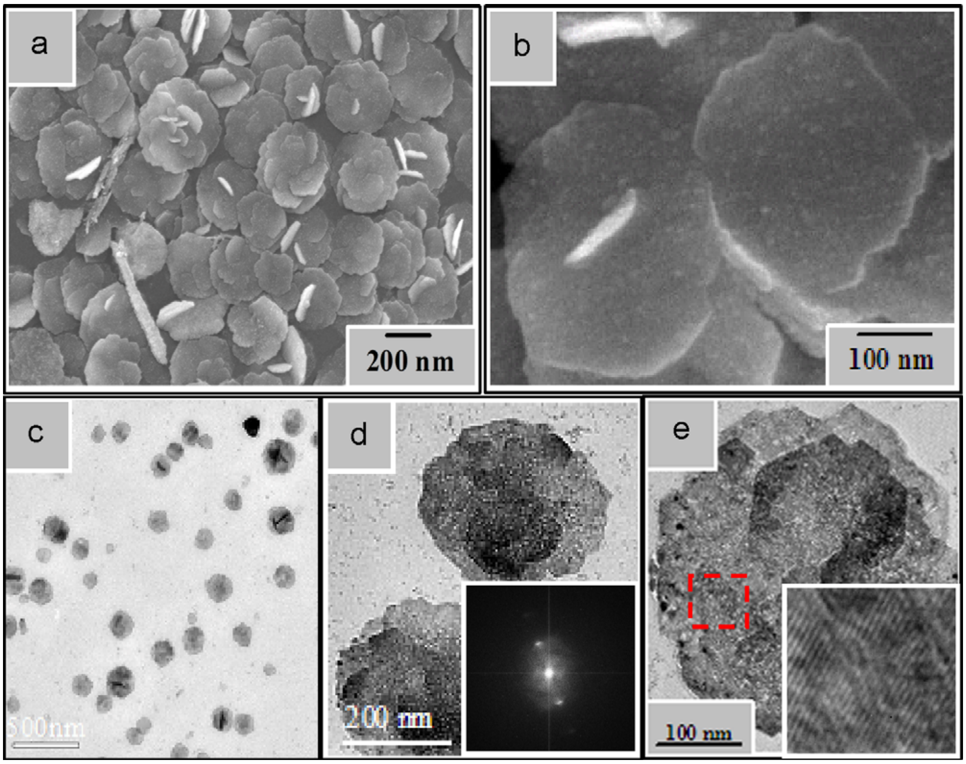

Fig. 2. (a) Low-magnification SEM image of the Cu_2O nanosheets. (b) Enlarged SEM image of the Cu_2O nanosheets. (c, d) TEM images of the Cu_2O nanosheets. (e) TEM image of an individual Cu_2O nanosheet.

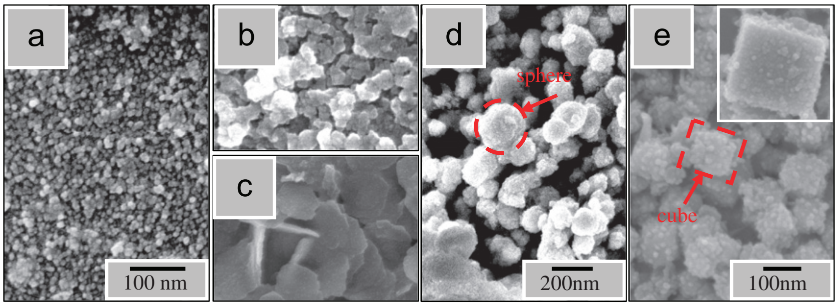

Fig. 3. SEM images. (a) Cu nanocolloids. (b, c) Time-dependent evolution of the sheetlike Cu_2O crystal morphology at different growth stages ((b) 30 min, (c) 60 min). (d, e) SEM images of Cu_2O nanostructures synthesized by different oxidants ((d) in water, (e) in acetone).

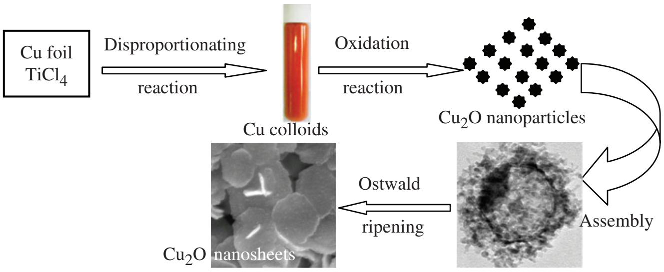

Fig. 4. Schematic illustration of the formation process of the 2D Cu_2O nanosheets.

a characteristic peak of strong absorbance at 580 nm is due to the surface plasmon band of Cu colloids [25]. As the oxidation reaction continued, the absorption band gradually shifted to red and the intensity decreased until it disappeared after 60 min. The red shift in the absorption with aging time may thus be attributed to an increase in the size of the crystals. The oxidation process was also accompanied by a color change from red to blue to green to yellow (Fig. 5b). For comparison, the different reaction systems have appeared as different UV–vis absorption spectroscopy during the oxidation process (Fig. 5c and d).

According to the equation $\alpha E_p = K(E_p - E_g)^{1/2}$ (where α is the absorption coefficient, E_p is the discrete photo energy, K is a constant, and E_g is the band gap energy) [26,27], a classical Tauc approach is further employed to estimate the E_g value of Cu_2O nanosheets. The plots of $(\alpha E_p)^2$ vs E_p based on the direct transition are shown in Fig. 6b. The extrapolated value (the lines to the x axis) of E_p at $\alpha = 0$ gives absorption edge energies corresponding to $E_g = 2.86$ eV. The value of nanosheets is apparently greater than the value of bulk Cu_2O, which is attributed to the quantum confinement effects arising from the tiny Cu_2O particles without any surfactant and additive [28].

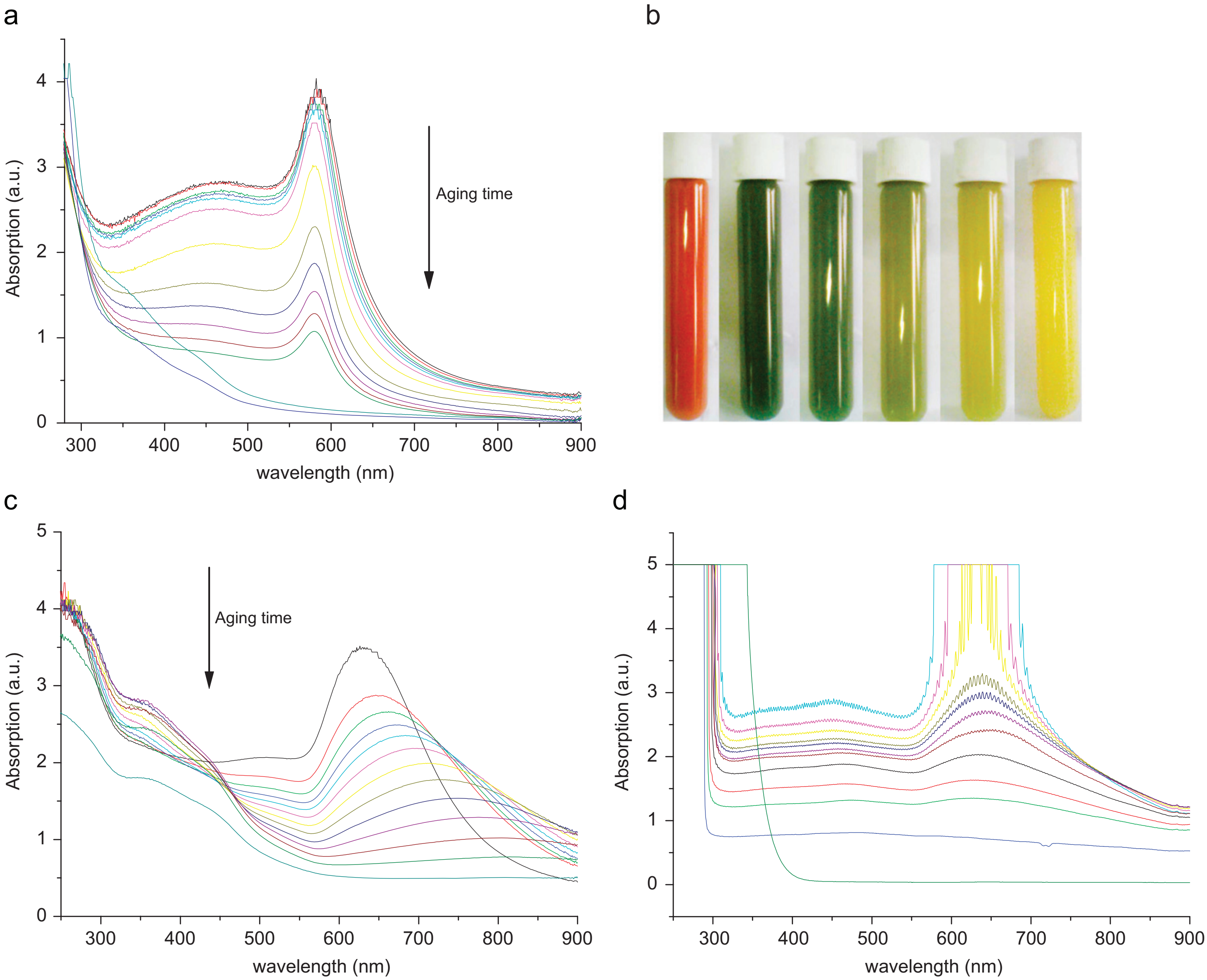

Fig. 5. UV–vis absorption spectra obtained over oxidation process of copper colloids. (a) In ethanol. (c) In H_2O. (d) In acetone. (b) Gives the color change of the oxidation process.

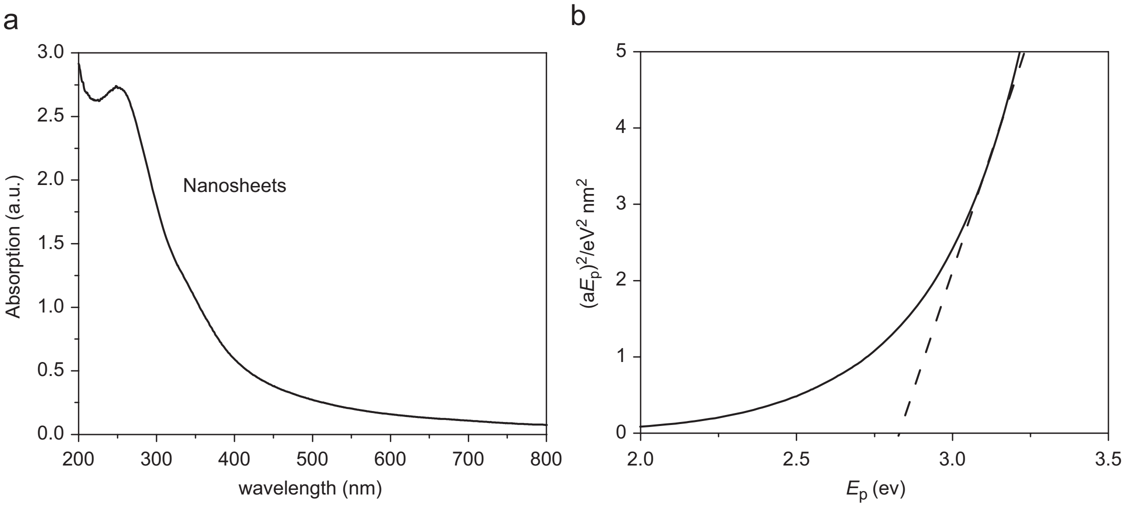

Fig. 6. (a) Typical UV–vis absorption spectra of the Cu_2O nanosheets. (b) $(\alpha E_p/eV)^2$ vs E_p corresponding curves of the products.

4. Conclusion

In summary, Cu_2O nanosheets were synthesized by using a novel, simple wet chemical route. It was demonstrated that the solvent agent of ethanol played key roles in the formation of the as-synthesized nanosheets. By choosing the different solvent agent to limit the oxidized processes, Cu_2O nanospheres and nanocubes could be selectively synthesized accordingly. At the same time, the nanosheets exhibited blue-shift absorption possibly due to the quantum-size effect. These nanostructures showed very porous, hierarchical, and unique morphology and thus can be potentially used for harvesting solar energy, optics, catalysis and sensors in the visible range. Moreover, these Cu_2O nanostructures may be useful in reinforcing composite materials or in further modifying other nanostructures.

Acknowledgments

The authors appreciate the support program for young and capable teachers in XinYang Normal University of China (2006). We also thank the Support program by Natural Science Foundation of Henan Educational Committee (2008A140010).

References

[1] J.T. Hu, T.W. Odom, C.M. Lieber, Acc. Chem. Res. 32 (1999) 435.
[2] G.R. Patzke, F. Krumeich, R. Nesper, Angew. Chem. 41 (2002) 2446.
[3] Y. Xia, P. Yang, Y. Sun, Y. Wu, B. Mayers, B. Gates, Y. Yin, F. Kim, Y. Yan, Adv. Mater. 15 (2003) 353.
[4] C.N.R. Rao, F.L. Deepak, G. Gundiah, A. Govindaraj, Prog. Solid State Chem. 31 (2003) 5.
[5] A.M. Morales, C.M. Lieber, Science 279 (1998) 208.
[6] Z.W. Pan, Z.R. Dai, Z.L. Wang, Science 29 (2001) 1947.
[7] L.F. Gou, C.J. Murphy, Nano Lett. 3 (2003) 231.
[8] Y.G. Sun, Y.N. Xia, Science 298 (2002) 2176.
[9] T.W. Ebbesen, P.M. Ajayan, Nature 358 (1992) 220.
[10] X.S. Fang, C.H. Ye, L.D. Zhang, J.X. Zhang, J.W. Zhao, P. Yan, Small 4 (2005) 422.
[11] H. Zhang, D.R. Yang, Y.J. Ji, X.Y. Ma, J. Xu, D.L. Que, J. Phys. Chem. B 108 (2004) 3955.
[12] G.Z. Shen, Y. Bando, C.C. Tang, D. Golberg, J. Phys. Chem. B 110 (2006) 7199.
[13] E. Hosono, S. Fujihara, T. Kimura, Electrochim. Acta 49 (2004) 2287.
[14] Y.B. Li, Y. Bando, D. Golberg, Appl. Phys. Lett. 82 (2003) 1962.
[15] R. Liu, E.A. Kulp, F.E. Oba, W. Bohannan, F. Ernst, J.A. Switzer, Chem. Mater. 17 (2005) 725.
[16] Y. Chang, J.J. Teo, H.C. Zeng, Langmuir 21 (2005) 1074.
[17] W.Z. Wang, G.H. Wang, X.S. Wang, Y.J. Zhan, Y.K. Liu, C.L. Zheng, Adv. Mater. 14 (2002) 67.
[18] Y. Xiong, Z. Li, R. Zhang, Y. Xie, J. Yang, C. Wu, J. Phys. Chem. B 107 (2003) 3697.
[19] W.T. Yao, S.H. Yu, Y. Zhou, J. Jiang, Q.S. Wu, L. Zhang, J. Jiang, J. Phys. Chem. B 109 (2005) 14011.
[20] R. Liu, F. Oba, E.W. Bohannan, F. Ernst, J.A. Switzer, Chem. Mater. 15 (2003) 4882.
[21] J.J. Teo, Y. Chang, H.C. Zeng, Langmuir 22 (2006) 7369.
[22] Y.S. Luo, S.Q. Li, Q.F. Ren, J.P. Liu, L.L. Xing, Y. Wang, Y. Yu, Z.J. Jia, J.L. Li, Cryst. Growth. Des. 7 (2007) 87.
[23] P. He, X. Shen, H. Gao, J. Colloid Interface Sci. 284 (2005) 510.
[24] H. Xu, W. Wang, W. Zhu, J. Phys. Chem. B 110 (2006) 13829.
[25] I. Lisiecki, M.P. Pileni, J. Phys. Chem. 99 (1995) 5077.
[26] M. Yin, C.K. Wu, Y. Lou, C.B. Burda, J.T. Koberstein, Y. Zhu, J. Am. Chem. Soc. 127 (2005) 9506.
[27] K. Borgohain, N. Murase, S. Mahamuni, J. Appl. Phys. 92 (2002) 1292.
[28] J.W. Zhu, H.Q. Chen, H.B. Liu, X.J. Yang, Lu, L.D.X. Wang, Mater. Sci. Eng: A 384 (2004) 172.